Dalton Transactions

Accepted Manuscript

This is an *Accepted Manuscript*, which has been through the Royal Society of Chemistry peer review process and has been accepted for publication.

Accepted Manuscripts are published online shortly after acceptance, before technical editing, formatting and proof reading. Using this free service, authors can make their results available to the community, in citable form, before we publish the edited article. We will replace this *Accepted Manuscript* with the edited and formatted *Advance Article* as soon as it is available.

You can find more information about *Accepted Manuscripts* in the Information for Authors.

Please note that technical editing may introduce minor changes to the text and/or graphics, which may alter content. The journal's standard Terms & Conditions and the Ethical guidelines still apply. In no event shall the Royal Society of Chemistry be held responsible for any errors or omissions in this *Accepted Manuscript* or any consequences arising from the use of any information it contains.

ROYAL SOCIETY OF CHEMISTRY

www.rsc.org/dalton

An Investigation of Zr Doping in $NaBiTi_2O_6$ Perovskite by Direct Hydrothermal Synthesis

Mohammad H. Harunsani,[1,†] David I. Woodward,[2] Pam A. Thomas[2] and Richard I. Walton[1,*]

[1]Department of Chemistry, University of Warwick, Coventry CV4 7AL, U.K.

*Author for correspondence: r.i.walton@warwick.ac.uk

[2]Department of Physics, University of Warwick, Coventry CV4 7AL, U.K.

† Present address: Universiti Brunei Darussalam, Faculty of Science, Jln. Tungku Link, Gadong, BE1410, Brunei Darussalam

Abstract

The direct crystallisation of perovskites $NaBi(Ti_{1-x}Zr_x)_2O_6$ with x = 0, 0.01, 0.05 and 0.1 at 240 °C is achieved from aqueous alkali (NaOH) solutions of $NaBiO_3$, TiF_3 and $ZrOCl_2$. For each material, a single rhombohedral polymorph (*R*3*c* *a* ~ 5.51 Å, *c* ~ 13.50 Å) can be fitted to powder X-ray diffraction data, with Rietveld refinement showing a linear increase in lattice parameters and unit cell volume with increasing Zr content. Scanning electron microscopy shows micron-sized cube-shaped crystallites for each sample, with energy-dispersive X-ray analysis giving Bi:Ti:Zr ratios consistent with the expected substitution. Raman spectroscopy shows no perturbance of local structure upon Zr doping and the spectrum shows five broad bands, consistent with the literature on similar materials. Attempts to increase the Zr content further (x > 0.1) were unsuccessful by this hydrothermal synthesis method, leading instead to crystalline ZrO_2 by-products. For $NaBiTi_2O_6$ and $NaBi(Ti_{0.99}Zr_{0.01})_2O_6$ densified ceramics were prepared (~ 95 % of crystallographic value) and the remnant polarisation was found to be reduced upon Zr substitution, with a higher maximum piezoelectric coefficient, d_{33}, measured and comparable permittivity and dielectric loss reported to other $NaBiTi_2O_6$ materials.

Dalton Transactions Accepted Manuscript

Introduction

The perovskite $NaBiTi_2O_6$ has been proposed and investigated as a lead-free alternative to the widely used $PbTi_{1-x}Zr_xO_3$ (PZT) perovskites that find commercial application because of their ferroelectric and piezoelectric properties in numerous electronic devices, such as actuators transducers, and sensors.[1] The crystal structure of $NaBiTi_2O_6$ was originally reported at ambient conditions as rhombohedral (space group *R*3*c*),[2] but more recent work using Raman spectroscopy,[3] single crystal X-ray diffraction[4] high-resolution powder diffraction,[5] and total neutron scattering[6] has assigned monoclinic symmetry (*Cc*). Some of these studies have reported the coexistence of the rhombohedral and monoclinic structures at room temperature, and Rao *et al.* reported that the relative amount of each is dependent on sample history (heating and mechanical treatment).[7] As well as ferroelectricity and piezoelectricity, Sinclair and co-workers have recently reported high-temperature oxide ion conductivity in $NaBiTi_2O_6$ comparable to the fluorite-type oxides such as yttrium-stabilised zirconia.[8] This effect is optimised by small adjustments in metal ratios that give oxide deficiency.

The addition of dopant metals to any perovskite oxide is a powerful means of controlling and optimising electronic and other properties, and a variety of dopants have been added to $NaBiTi_2O_6$.[9] Only last year Blanchard *et al.* reported a comprehensive study of the effect of B-site Zr doping in $NaBiTi_2O_6$ in terms of the crystal chemistry of the resulting phases.[10] The aims of their work were to clarify some of the literature in the field concerning the evolution of crystal structure with composition and to explore the possible existence of a morphotropic phase boundary by analogy to PZT, where the coexistence of two or more ferroelectric phases can give enhanced piezoelectric response, although they did not report any property measurements.

Sample homogeneity and precise control of stoichiometry is important in the electronic properties of all materials, not only to ensure reproducibility for practical applications, but also to establish correct structure-property relationships for fundamental understanding of the origin of properties. Carter *et al.* recently explored the effect of non-stoichiometry in $NaBiTi_2O_6$ and found that small adjustments in Na and Bi content away from the ideal composition had a detrimental effect on ferroelectric hysteresis and

Dalton Transactions Accepted Manuscript

piezoelectric coefficients.[11] From a materials synthesis and processing viewpoint, homogeneity of $NaBiTi_2O_6$ is not easy to achieve, since bismuth oxide, and to a lesser extent sodium oxide, are highly volatile. Thus in any high-temperature preparative method, loss of reagents occurs easily and precautions must be taken to contain this potential source of sample irreproducibility.[12, 13] Alternative synthesis methods for these materials that use low reaction temperatures and, particularly, solution-mediated crystallisation are thus desirable. Although co-precipitation, such as the Peccini method, and other related sol-gel processing methods use ambient temperature precipitation of homogeneous solids, treatment at several hundred degrees is still needed to induce crystallisation,[14] which may still result in loss of intended substituents when multi-element mixed oxides are being studied. Direct crystallisation from solution using hydrothermal, or more generally solvothermal conditions, is thus desirable as a 'one pot' synthesis approach to complex oxides, with the closed conditions preventing loss of reagents to the atmosphere, while the low reaction temperatures (typically around 200 °C) and use of solutions enable some control over crystal morphology and potentially the chemistry of the phase produced.[15] The hydrothermal synthesis of a number of perovskite materials has now been reported, including ferroelectric titanates and niobates, magnetoresitive manganites and multiferroic chromites.[16] For example, Handoko and Goh prepared complex thin films by hydrothermal synthesis based on $(Na,K)NbO_3$-$LiTaO_3$ solid solutions that showed piezoelectric activity after heat treatment at only 600 °C, thus avoiding loss of volatile potassium.[17]

The hydrothermal synthesis of $NaBiTi_2O_6$ has been reported by a number of groups, using highly alkali solutions and a variety of Ti and Bi-containing precursors, [18, 19, 20] while Li *et al.* used citric acid as an additive in hydrothermal reactions as a means of modifying crystal size and shape of the material.[21] In this paper we consider the hydrothermal formation of Zr-doped $NaBiTi_2O_6$, a system not previously studied using this synthesis method, with the aim of investigating how electroceramics with favourable properties may be formed from the fine polycrystalline powder produced, and compare our results with the recent crystal chemistry study published by Blanchard and co-workers

Dalton Transactions Accepted Manuscript

and with the electronic properties reported for other titanate perovskites formed by hydrothermal synthesis.

Experimental Section

Hydrothermal syntheses were performed using 45 mL Teflon-lined stainless steel autoclaves (Parr 4744). Stoichiometric amounts of $NaBiO_3 \cdot 2H_2O$ (Acros, 85%), TiF_3 (Alfa, 98%) and $ZrOCl_2 \cdot 8H_2O$ (Sigma Aldrich, 99.5%) were weighed to give products of intended composition $NaBi(Ti_{1-x}Zr_x)_2O_6$ with x = 0, 0.01, 0.05 and 0.1, using 0.6320 g of $NaBiO_3 \cdot 2H_2O$. The water contents of all salts were determined using thermogravimetric analysis to allow accurate weighing. The reagents were mixed in 2 mL deionised water for 5 min in the Teflon liner before 18 mL of NaOH solution was added and stirred so that the final NaOH concentration was 10 M. The reaction mixture was then stirred for 1 hour before it was sealed in a steel autoclave and placed in an oven pre-heated at 240 ^{o}C. After heating for 4 days, the autoclaves were left to cool naturally to room temperature. The solid products were recovered by suction filtration, washed thoroughly with warm water and dried overnight at 70 ^{o}C in a drying oven. The products were then ground into powder for further characterisation.

Powder X-ray diffraction (XRD) patterns were recorded at room temperature using a Panalytical X'Pert Pro MPD operating with monochromatic Cu $K\alpha_1$ radiation and equipped with a PIXcel solid-state detector. Full pattern analysis of powder patterns was performed using the Rietveld method within the TOPAS software.[22] SEM images of the samples were recorded using Zeiss SUPRA 55VP FEG scanning electron microscope. A working distance of 3 mm and a gun voltage of 20 kV were used. Energy Dispersive X-ray Analysis (EDXA) was also performed within the SEM using an EDAX Genesis analytical system with thin window detector, in order to determine the elemental composition of the materials. Raman spectroscopic data were recorded at room temperature using a Renishaw inVia Raman Microscope equipped with an Ar^+ laser with wavelength 514.5 nm and Renishaw CCD detectors.

Dalton Transactions Accepted Manuscript

Samples that were investigated for their dielectric properties were first pressed into a pellet of diameter 13 mm using a load of 2 tonnes. Approximately 1 g of powder was used to make each pellet. The pellets were placed on Pt foil, covered with an alumina crucible and heated to 1100 ^{o}C for 2 hours at a heating rate of 5 ^{o}C min^{-1}. After being left to cool to room temperature, a second heating at 1150 ^{o}C for 4 hours was carried out. The mass, thickness and diameter of the pellets were then measured to determine their density. Silver paint was then applied on both faces of the pellet for dielectric and piezoelectric measurements. The pellets were poled by placing them in silicone oil and applying a fixed voltage for 1 minute. The longitudinal piezoelectric coefficient, d_{33}, was then measured at 5 different points on each sides of the pellet using a YE2730A d_{33} meter. An average and standard deviation of these values was then calculated. Dielectric hysteresis measurement was studied on pellets immersed in silicone oil using a triangular waveform at a frequency of 50 mHz. The peak voltage was increased until a current peak associated with the coercive field was observed. Data were collected using Labview software. The dielectric permittivity and loss of the pellets were measured at frequencies of 1 kHz, 10 kHz, 100 kHz and 1 MHz using a HP 4192 A LF Impedance Analyser at a heating rate of 60 ^{o}C h^{-1} from 30 to 600 ^{o}C.

Results and Discussion

Perovskites of composition $NaBi(Ti_{1-x}Zr_x)_2O_6$ with x = 0, 0.01, 0.05 and 0.1 could be prepared using the hydrothermal synthesis approach we adopted. Note that this method differs from most previous hydrothermal synthesis conditions in that we used $NaBi^{V}O_3{\cdot}2H_2O$ as an oxidant and $Ti^{III}F_3$ as reductant, with the aim of achieving atomic-scale homogeneity of the metal cations in the oxide product.[19] Figure 1 shows powder XRD patterns of the three Zr-containing samples along with an undoped $NaBiTi_2O_6$ sample made by the same method. The structural parameters from Rietveld refinement using a single phase fit in space group *R*3*c* gave the structural parameters shown in Table 1. Although, as discussed in the Introduction, monoclinic symmetry has been assigned to $NaBiTi_2O_6$, Aksel *et al.* pointed out that the monoclinic distortion is only apparent after the samples have been annealed and the subtle changes in powder diffraction profile on symmetry lowering can easily be

Dalton Transactions Accepted Manuscript

obscured by sample-dependant peak broadening.[5] Furthermore it is conceivable that the sample preparation method dictates which crystal symmetry is found, or at least the proportion of phases present in the product mixture.[7] Thus it is not unexpected that for our samples we found that lower symmetry spacegroups gave no improvement in fit and for comparison purposes it is also convenient to use the rhombohedral symmetry. The lattice parameters *a* and *c* show a linear increase with increasing Zr content over the limited composition range that this method allows, and these are plotted on Figure 2, along with the same values reported by Blanchard *et al.* for materials prepared using a high-temperature annealing method.[10] Blanchard *et al.* found that for their samples, prepared by annealing at 800 °C, for Zr content of up to x = 0.2 the high-resolution powder XRD was best fitted as a mixture of rhombohedral and monoclinic phases with increasing proportion of the rhombohedral phase with Zr content. The points on Figure 2 are those of the rhombohedral component. It can be seen that the absolute values give moderate agreement between those from our samples and the data of Blanchard *et al.*, and the differences may possibly be due to the actual level of Zr inclusion. But importantly, the trend of increasing lattice parameters with Zr content is very similar in each case. Attempts to include larger amounts of Zr in our hydrothermal synthesis lead to solid products contaminated with crystalline ZrO_2, and similarly the pure zirconium analogue of the material could not be prepared using this hydrothermal method. This suggests there is a limitation to the amount of Zr that can be included into $NaBiTi_2O_6$ by hydrothermal crystallisation.

The Raman spectra of $NaBi(Ti_{1-x}Zr_x)_2O_6$ shown in Figure 3 agree well with previous Raman studies of $NaBiTi_2O_6$. From group theory, $NaBiTi_2O_6$ is expected to have 13 Raman active modes, $7A_1 + 6E$.[23] However, the spectra observed for all three samples show only five broad bands. This reduction in the number of observed modes may be due to the overlapping of multiple Raman modes and the broadening of the peaks due to the disorder on both the A-site and B-site. The addition of Zr clearly has very little effect on the Raman spectra of $NaBiTi_2O_6$ at the concentrations studied in the present work. The hydrothermal synthesis of $NaBi(Ti_{1-x}Zr_x)_2O_6$ gave cubic particles which are 2-4 μm in size as shown Figure 4. The atomic composition was determined by EDXA and the presence of Zr

Dalton Transactions Accepted Manuscript

was confirmed in the doped samples, with the calculated Zr content similar to the expected values (Table 2).

Polarisation hysteresis for $NaBi(Ti_{1-x}Zr_x)_2O_6$ is shown in Figure 5a. A hysteresis loop is observed for $NaBiTi_2O_6$ and x = 0.01 but on the addition of Zr at x = 0.05 and x = 0.1, the loop loses the inflection feature that identifies it as ferroelectric. This may result from either a composition-dependent phase transition to a non-ferroelectric structure or from the coercive field increasing to a value above the limit of this experiment. The result is that the loop becomes elliptical and the remnant polarisation (polarisation at zero field) is reduced with increasing Zr substitution. This trend is similar to the results obtained by Rachakom *et al.* where elliptical loops were observed for $NaBi(Ti_{1-x}Zr_x)_2O_6$ with Zr concentration between $0.2 \leq x \leq 0.8$.[24]

The piezoelectric coefficient, d_{33} of $NaBi(Ti_{1-x}Zr_x)_2O_6$ is shown in Figure 5 plotted against the electric field applied on poling. For undoped $NaBiTi_2O_6$, x = 0.01 and x = 0.05 showed a hysteresis loop as the poling field was varied. This was not the case for x = 0.1, and no hysteresis loop was obtained due to the sample breaking down electrically during poling. The mean maximum d_{33} values of each material are shown in Table 2, along with the measured densities of the pellets studied. The measurement of a reversible d_{33} up to x = 0.1 demonstrates that some ferroelectric character is present in all samples and therefore the elliptical appearance of the hysteresis loops in Figure 5a is due to the dielectric breakdown of the ceramics at an electric field below the coercive field for these samples. Although the maximum d_{33} for all samples is recorded at x = 0.01, this may not represent the true maximum across the series, as the pellets with x = 0.05 and 0.1 had low densities that significantly lower the d_{33} that is measured. The inability to densify the higher Zr content perovskites under identical conditions to the other samples may be due to Zr^{4+} inhibiting the solid-state diffusion or recrystallisation processes necessary for densification. While higher temperatures would be expected to yield higher densities, volatilisation of Bi and Na becomes significant, potentially leading to the appearance of secondary phases. For the $NaBiTi_2O_6$ sample, the measured d_{33} is typical of many other samples of the perovskite that have been reported for materials prepared by a variety of

Dalton Transactions Accepted Manuscript

methods: for example solid state synthesis (d_{33} = 68 pC N^{-1})[25] and hydrothermal synthesis with different reagents (d_{33} = 53 pC N^{-1}).[20] It is interesting to note that the replacement of just 1% of Ti by Zr gives an increased value of d_{33}, a phenomenon which is also seen with A-site substitutions such as Ba[26] or K.[27] B-site substitutions of Mn^{3+} and Fe^{3+} over a similar range have been shown to result in a lowering of the d_{33} of ceramics,[28] although as these have a lower valance than the Ti^{4+} ions that they replace, oxygen vacancies are also introduced that will have additional effects on the electrical behaviour. It can be speculated that the addition of Zr assists in locally stabilising more directions for the polarisation vectors, leading to an increase in the ceramic d_{33}. A concurrent reduction in the magnitude of the polarisation vector can explain both the reduction in the remnant polarisation and the anticipated peak in d_{33} across the series.

Permittivity and dielectric loss of the $NaBi(Ti_{0.99}Zr_{0.01})_2O_6$ are shown in Figure 6. The maximum relative permittivity is observed at ~360 °C with a value of 2450 which is comparable to values reported for solid-state $NaBiTi_2O_6$ (~3400)[29] or hydrothermal $NaBiTi_2O_6$ in the literature (~2800).[20] The overall shape of these curves is very similar to other $NaBiTi_2O_6$ reported in the literature. Hiruma *et al.* studied the permittivity of $NaBiTi_2O_6$ ceramics with variable stoichiometries [13] and the data presented here for $NaBi(Ti_{0.99}Zr_{0.01})_2O_6$ appear most similar to those where the proportion of Bi slightly exceeds that of Na as these are seen to have low losses up to higher temperatures than when Na is in higher proportion than Bi. This may indicate a small preference of the structure for a slight excess of the larger Bi ion as the unit cell expands, but this level of non-stiochiometry is not detected in the analysis we have made.

Conclusions

A hydrothermal synthesis method allows low concentrations of Zr to be introduced into the ferroelectric perovskite $NaBiTi_2O_6$. Although the method cannot be used to prepare a complete solid solution, the polycrystalline powder formed can be effectively sintered into a dense ceramic for the case of $NaBi(Ti_{0.99}Zr_{0.01})_2O_6$. This produces a material with enhanced polarisation hysteresis and

Dalton Transactions Accepted Manuscript

piezoelectric response compared to the undoped, parent material prepared by the same method, and overall characteristics that match the literature on $NaBiTi_2O_6$ prepared using conventional ceramic syntesis methods.

Acknowledgments

MHH thanks the Ministry of Education, Brunei for award of a scholarship. Some of the equipment used in materials characterisation at the University of Warwick was obtained through the Science City Advanced Materials project "Creating and Characterising Next Generation Advanced Materials" with support from Advantage West Midlands (AWM) and part funded by the European Regional Development Fund (ERDF). We are grateful to Mr Luke Daniels for his assistance with some of the powder XRD analysis.

Dalton Transactions Accepted Manuscript

Table 1: Refined structural parameters and *R*-factors of $NaBi(Ti_{1-x}Zr_x)_2O_6$ from Rietveld analysis of XRD. Note that occupancies were fixed at values expected from synthesis and elemental analysis.

Sample	x = 0	x = 0.01	x = 0.05	x = 0.1
Space group	*R*3*c*	*R*3*c*	*R*3*c*	*R*3*c*
***a* = *b* /Å**	5.5015(13)	5.5050(10)	5.5162(6)	5.5341(17)
***c* /Å**	13.487(6)	13.495(3)	13.523(3)	13.548(8)
Cell volume / Å^3	353.5(4)	354.18(13)	356.36(8)	359.3(4)
Na/Bi (*x,y,z*)	(0,0,0.264(2))	(0,0,0.266(2))	(0,0,0.261(2))	(0,0,0.275(2))
Ti/Zr (*x,y z*)	(0,0,0.018(2))	(0,0,0.020(2))	(0,0,0.016(3))	(0,0,0.016(3))
O (*x,y,z*)	(0.163(4),0.387(6), 0.0833)	(0.160(4),0.380(6), 0.0833)	(0.153(6),0.369(9), 0.0833)	(0.153(3),0.369(5), 0.0833)
Fractional Occupancy				
Na	0.5	0.5	0.5	0.5
Bi	0.5	0.5	0.5	0.5
Ti	1	0.99	0.95	0.9
Zr	-	0.01	0.05	0.1
O	1	1	1	1
R_{wp}	15.231	16.255	14.913	15.223
R_p	12.052	12.683	11.524	11.836
Gof	1.310	1.696	1.263	1.289
B_{iso} / Å^2				
Na	5.92(16)	7.7 (2)	6.76 (2)	7.03(18)
Bi	5.92(16)	7.7(2)	6.76(2)	7.03(18)
Ti	0.80(12)	0.19(14)	0.69(15)	0.12(9)
Zr	-	0.19(14)	0.69(15)	0.12(9)
O	0.3(4)	0.9(3)	0.2(4)	0.4(3)

Table 2: Atomic composition of $NaBi(Ti_{1-x}Zr_x)_2O_6$ obtained from EDXA. Expected values are in brackets.

Zr conc., x (Nominal value)	Na / %	Bi / %	Zr / %	Ti / %	Zr conc. measured
0	10.9 (10)	10.9 (10)	-	21.8 (20)	0
0.05	10.6 (10)	8.6 (10)	0.6 (1)	16.3 (19)	0.04
0.1	9.7 (10)	9.3 (10)	1.8 (2)	15.0 (18)	0.11

Table 3: Piezoelectric coefficient, d_{33}, and relative density of $NaBi(Ti_{1-x}Zr_x)_2O_6$. Note: Relative density was calculated from observed density/crystallographic density

x in $NaBi(Ti_{1-x}Zr_x)_2O_6$	Maximum mean d_{33} / pC N^{-1}	Relative density / %
0	61.9 ± 1.1	95.0
0.01	79.7 ± 1.3	95.2
0.05	7.1 ± 0.7	79.9
0.1	0.5 ± 0.2	77.8

Dalton Transactions Accepted Manuscript

Figure Captions

Figure 1: Results of Rietveld refinement of powder X-ray diffraction data of $NaBi(Ti_{1-x}Zr_x)_2O_6$ for (a) x = 0, (b) x = 0.01, (c) x = 0.05 and (d) x = 0.1 refined with space group *R*3*c* (see Table 1 for refined structural parameters).

Figure 2: Rhombohedral lattice parameter *vs* composition for $NaBi(Ti_{1-x}Zr_x)_2O_6$. The filled symbols are those for the hydrothermal samples prepared in the current work and the open symbols are those reported by Blanchard *et al.* for samples prepared by solid-state synthesis.[10]

Figure 3: Raman spectra of $NaBi(Ti_{1-x}Zr_x)_2O_6$ with increasing Zr concentration.

Figure 4: SEM images of $NaBi(Ti_{1-x}Zr_x)_2O_6$ for (a) x = 0, (b) x = 0.01, (c) x = 0.05 and (d) x = 0.1.

Figure 5: (a) Polarisation hysteresis and (b) piezoelectric coefficient, d_{33} measured for pelletised and annealed samples of $NaBi(Ti_{1-x}Zr_x)_2O_6$

Figure 6: Permittivity and dielectric loss curves of $NaBi(Ti_{0.99}Zr_{0.01})_2O_6$ at frequencies 1 kHz, 10 kHz, 100 kHz and 1 MHz measured upon cooling from 570-40 ^oC

References

1. G. H. Haertling, *J. Amer. Ceram. Soc.*, 1999, **82**, 797; T. R. Shrout and S. J. Zhang, *J. Electroceram.*, 2007, **19**, 113.
2. J. A. Zvirgzds, P. P. Kapostinš, J. V. Zvirgzde and T. V. Kruzina, *Ferroelectrics*, 1982, **40**, 75; G. O. Jones and P. A. Thomas, *Acta Crystallogr. Sect. B-Struct. Sci.*, 2002, **58**, 168.
3. J. Petzelt, S. Kamba, J. Fabry, D. Noujni, V. Porokhonskyy, A. Pashkin, I. Franke, K. Roleder, J. Suchanicz, R. Klein and G. E. Kugel, *J. Phys.-Condens. Matter*, 2004, **16**, 2719.

Dalton Transactions Accepted Manuscript

4. S. Gorfman and P. A. Thomas, *J. Appl. Crystallogr.*, 2010, **43**, 1409.

5. E. Aksel, J. S. Forrester, J. L. Jones, P. A. Thomas, K. Page and M. R. Suchomel, *Appl. Phys. Lett.*, 2011, **98**, 3.

6. E. Aksel, J. S. Forrester, J. C. Nino, K. Page, D. P. Shoemaker and J. L. Jones, *Phys. Rev. B*, 2013, **87**, 10.

7. B. N. Rao, A. N. Fitch and R. Ranjan, *Phys. Rev. B*, 2013, **87**, 5.

8. M. Li, M. J. Pietrowski, R. A. De Souza, H. R. Zhang, I. M. Reaney, S. N. Cook, J. A. Kilner and D. C. Sinclair, *Nat. Mater.*, 2014, **13**, 31.

9. J. R. Gomah-Pettry, E. Said, P. Marchet and J. P. Mercurio, *J. European Ceram. Soc.*, 2004, **24**, 1165.

10. P. E. R. Blanchard, S. Liu, B. J. Kennedy, C. D. Ling, Z. Zhang, M. Avdeev, L.-Y. Jang, J.-F. Lee, C.-W. Paoe and J.-L. Chene, *Dalton Trans.*, 2014, **43**, 17358.

11. J. Carter, E. Aksel, T. Iamsasri, J. S. Forrester, J. Chen and J. L. Jones, *Appl. Phys. Lett.*, 2014, **104**, 4.

12. Y. S. Sung, J. M. Kim, J. H. Cho, T. K. Song, M. H. Kim and T. G. Park, *Appl. Phys. Lett.*, 2011, **98**, 3.

13. Y. Hiruma, H. Nagata and T. Takenaka, *J. Appl. Phys.*, 2009, **105**, 8.

14. J. Gopalakrishnan, *Chem. Mat.*, 1995, **7**, 1265.

15. M. Yoshimura, *J. Mater. Res.*, 1998, **13**, 796; G. Demazeau, *J. Mater. Chem.*, 1999, **9**, 15; R. E. Riman, W. L. Suchanek and M. M. Lencka, *Ann. Chim.-Sci. Mat.*, 2002, **27**, 15.

16. D. R. Modeshia and R. I. Walton, *Chem. Soc. Rev.*, 2010, **39**, 4303.

17. A. D. Handoko and G. K. L. Goh, *CrystEngComm*, 2013, **15**, 672.

18. M. M. Lencka, M. Oledzka and R. E. Riman, *Chem. Mat.*, 2000, **12**, 1323; N. Kumada, Y. Morozumi, Y. Yonesaki, T. Takei, N. Kinomura and T. Hayashi, *J. Ceram. Soc. Jpn.*, 2008, **116**, 1238.

19. K. Sardar and R. I. Walton, *J. Solid State Chem.*, 2012, **189**, 32.

Dalton Transactions Accepted Manuscript

20. A. O'Brien, D. I. Woodward, K. Sardar, R. I. Walton and P. A. Thomas, *Appl. Phys. Lett.*, 2012, **101**, 4.

21. J. Li, G. Wang, H. Wang, C. Tang, Y. Wang, C. Liang, W. Cai and L. Zhang, *J. Mater. Chem.*, 2009, **19**, 2253.

22. A. Coelho, *TOPAS-Academic V5, Coelho Software* 2012.

23. J. Kreisel, A. M. Glazer, G. Jones, P. A. Thomas, L. Abello and G. Lucazeau, *J. Phys.-Condens. Matter*, 2000, **12**, 3267.

24. A. Rachakom, P. Jaiban, S. Jiansirisomboon and A. Watcharapasorn, *Nanoscale Res. Lett.*, 2012, **7**, 5.

25. O. Elkechai, M. Manier and J. P. Mercurio, *Physica Status Solidi a-Applied Research*, 1996, **157**, 499.

26. T. Takenaka, K. Maruyama and K. Sakata, *Jap. J. Appl. Phys.*, 1991, **30**, 2236.

27. M. Otoničar, S. D. Skapin, M. Spreitzer and D. Suvorov, *J. European Ceram. Soc.*, 2010, **30**, 971.

28. M. Davies, E. Aksel and J. L. Jones, *J. Amer. Ceram. Soc.*, 2011, **94**, 1314.

29. S. Said and J. P. Mercurio, *J. European Ceram. Soc.*, 2001, **21**, 1333.

Dalton Transactions Accepted Manuscript

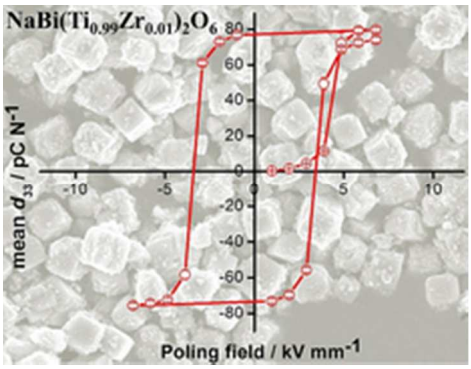

19x15mm (300 x 300 DPI)

Dalton Transactions Accepted Manuscript

Hydrothermal synthesis produces polycrystalline $NaBi(Ti_{1-x}Zr_x)O_6$ with small composition range; densified x = 0.01 material shows favourable piezoelectric coefficient and permittivity.

Dalton Transactions Accepted Manuscript